3
Trends and Advances in Cryogenic Materials

R.P. REED
Cryogenic Materials, Inc., Boulder, CO, 80305 USA

Abstract

Increased emphasis has been placed on research and development of specialized materials for use in low-temperature applications. Most research has been driven by (1) the construction of large superconducting coils, (2) requirements for transport and storage of liquefied natural gas, and (3) the discovery of superconductors with critical temperatures T_c as high as 90 K. The integration between structural design and material properties for critical low-temperature applications has been facilitated by the incorporation of fracture mechanics concepts. This development has led to measurement of an entirely new set of mechanical properties at low temperatures, to increased nondestructive inspection to measure in-situ flaw sizes, and to the development of fracture control practices for a number of cryogenic applications.

3.1 Introduction

To provide focused dissemination of new low-temperature-materials property information, the International Cryogenic Materials Conference (ICMC) was formed in 1974. The conference provided the only means for presenting and discussing the research and development of low-temperature structural metals and alloys and their welds, structural composites, and electrical and thermal insulators, as well as the application of fracture mechanics to inspection, properties, and design for cryogenic structures. And, since it held its meetings in parallel with the Cryogenic Engineering Conference, it provided an opportunity for synergistic interactions between cryogenic engineers and cryogenic materials specialists.

For discussion of cryogenic materials research over the past several decades, this paper is divided into two parts, namely overall trends and more significant specific technological advances. In the discussion of overall trends, the papers published in the ICMC proceedings are used to provide quantitative comparisons of variables, such as the origins of the research from various laboratories and worldwide and US trends. The trends of the focus of research (such as on structural alloys, composites,

or superconductors) are categorized over this time period. The use of the ICMC proceedings is thought to be a representative source for quantitative estimates of the trends in low-temperature materials (other than superconductors) research since they represent the only source, worldwide, that is focused on this subject. On the other hand, the general trends of research presented on superconductors in the ICMC proceedings may be skewed, since there are other conferences, of equivalent or larger size, on applied superconductivity and specialized workshops on high-T_c superconductors.

The second part of this review covers the technological advances that are related to materials at low temperatures. Since other review papers in this book focus on achievements related to superconductors, and since the author's interests have been directed toward structural alloy and composite development and characterization, this part emphasizes advancements in nonsuperconducting materials.

3.2 Trends in Cryogenic Materials Research

To quantify the overall trends of cryogenic materials research related to origins of the research, both worldwide and locally in the US, and the types of material studied, the number of papers in each volume of the proceedings of the biannual ICMC conferences held in the US and Canada for the past 30 years are tabulated. Two factors affect the correlation between the number of papers published in each of the proceedings and the number of papers actually presented at each conference: (1) not all speakers chose to prepare papers and (2) a modest number (~5%) of submitted papers have been rejected. It is doubtful that these variables will result in skewed results of the trends presented in this section.

Over the past 30 years, the number of papers included in the ICMC proceedings in volumes 22 to 52 (even-numbered volumes only) from 1975 to the present [1] have increased from about 60 during the two early, formative conferences. The number peaked at nearly 190 papers in 1995, and currently it is about 150 papers. This trend is illustrated in Figure 3.1. The decline from the conference in 2003 is likely caused by the less accessible location of the conference, i.e. Alaska.

The contributions from the US and Canada, Europe including Russia (RF) and Ukraine (Ukr), and Asia plus Australia to each of these proceedings are shown in Figure 3.2. In some cases, the conference location or timing of the conference has affected attendance from particular parts of the world. But, if averaged over the last six conferences, the US and Canada have contributed about 40% of the papers, Asia and Australia about 38%, and Europe including RF and Ukr 22%. Thus, the contributions of the US and Canada and Asia and Australia are almost equivalent, despite the fact that all the conferences have been held in the US and Canada. Over the entire 30-year period, these data indicate a slight increase in low-temperature R&D from the US and Canada and Europe including RF and Ukr, but a much greater increase in Asia plus Australia. This large increase correlates well with the strong increases in technological growth and gross national product of many of the Asiatic countries during this time period.

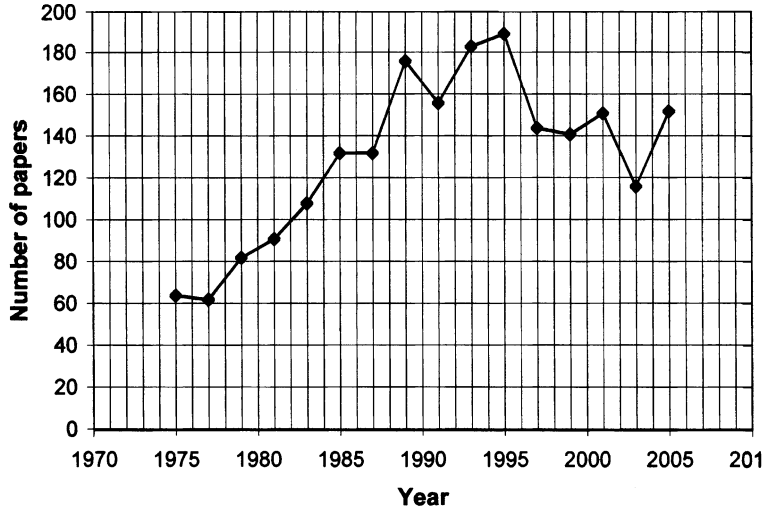

FIGURE 3.1. Total number of ICMC papers from 1975 through 2005.

Figure 3.3 presents the distribution of papers related to the types of material that were studied. The material classes used for this presentation include structural alloys (structural metals and alloys), composites/insulators (structural composites, thermal and electrical insulators, resins), functional (regenerator materials, normal-metal conductors, shape-memory alloys, others), and high- and low-T_c

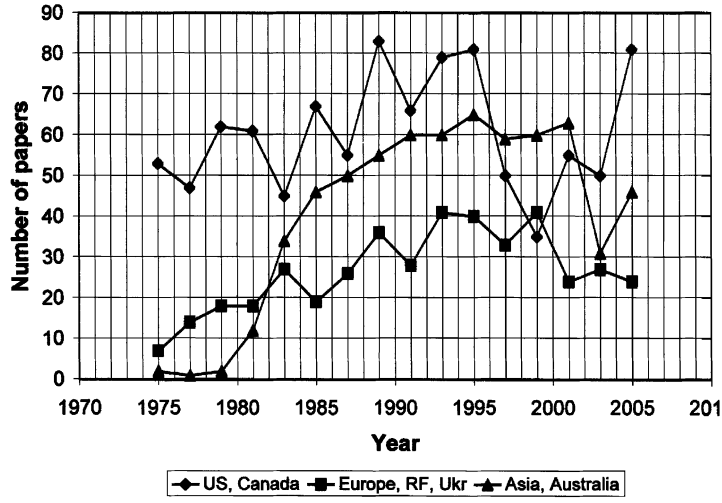

FIGURE 3.2. Geographical distribution of first authors of all ICMC papers from 1975 to 2005.

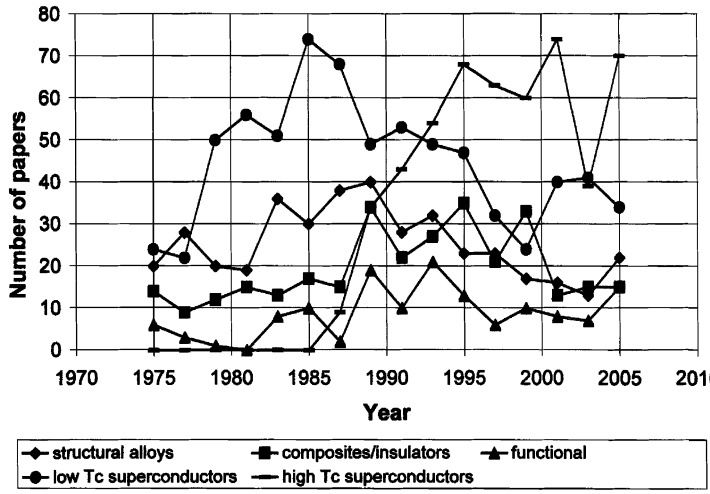

FIGURE 3.3. Topical distribution of all ICMC papers from 1975 to 2005.

superconductors. Obviously, there was a sudden and large emphasis in the R&D related to high-T_c superconductors after their discovery in 1986. Research on other material classes has increased slightly or remained constant. However, since the 1985–1989 time period, emphasis on low-T_c superconductors, structural alloys, and composite/insulator materials has steadily declined.

When we consider only three material categories (superconductors, structural alloys/composites, functional), their relative trends are easily recognizable (Figure 3.4). Emphasis on superconductors has continued to increase, functional

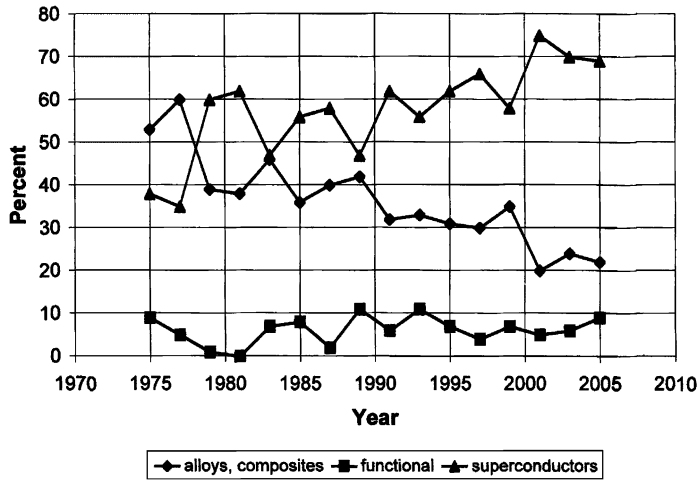

FIGURE 3.4. Very general topical distribution of all ICMC papers from 1975 to 2005.

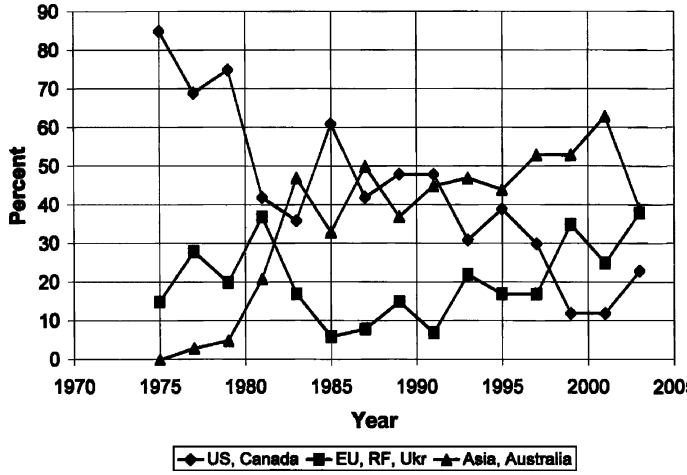

FIGURE 3.5. Geographical distribution of ICMC papers on structural alloys from 1975 to 2003.

material studies remain about constant, and emphasis on alloys and composites has declined. These trends represent the perception that additional studies related to superconductivity are likely to be more productive than gradual improvement of structural materials and insulation. The relative trends of the major continental areas for research on structural metals and alloys are shown in Figure 3.5. Note the ever-decreasing pattern of US contributions. Since about 1985, contributions from both Europe and Asia have gradually increased. Very similar 30-year trends are found in research contributions on composites (structural composites, electrical and thermal insulation and resins) shown in Figure 3.6. If we consider only the past 20 years, it is evident that all geographical sectors have contributed about equally and constantly over this period of time. Thus, since Europe and Asia have made equivalent contributions over the past 20 years, we may conclude that the US no longer dominates research on structural metals and alloys and composites. In fact, since all ICMC conferences have been held in the US or Canada, scientists from overseas are less likely to attend. This suggests that more R&D is currently being performed in Europe and Asia than in the US on these topics.

Figure 3.7 depicts the relative trends of US studies in alloys (structural metals and alloys), composites (structural composites, electrical and thermal insulation, resins) and superconductors (high and low T_c). The contributions on functional materials are omitted from this figure; these contributions have remained constant at about 10% over the time span considered. Quite clearly, as indicated in the overall projections, research has been increasing in superconductors and decreasing in alloys and composites. Now, over three times more research is presented on superconductors than on alloys and composites. Since ICMC is typically the only international conference used for the presentation of low-temperature alloy and composite information but is the smallest of several conferences for the

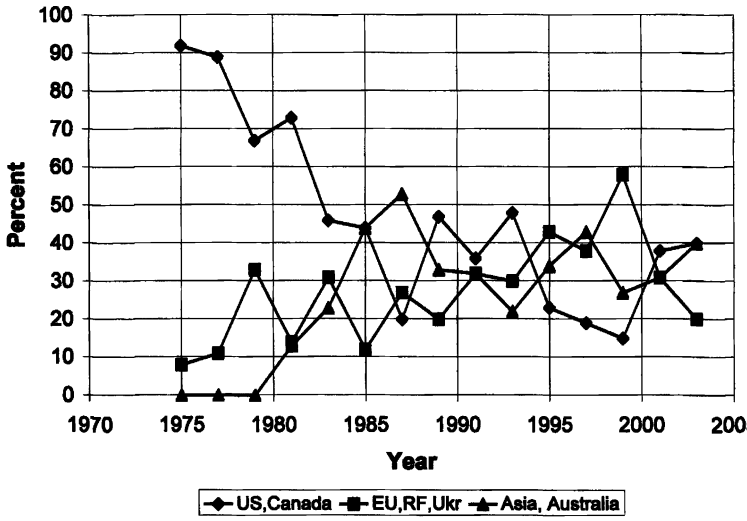

FIGURE 3.6. Geographical distribution of ICMC papers on composites from 1975 to 2003.

presentation of research on superconductors, the ratio of superconductor to alloys plus composite papers may be an order of magnitude greater, perhaps 35:1. Figure 3.7 suggests that this ratio continues to increase.

The relative contributions of government laboratories, industry, and universities to all cryogenic materials research are plotted in Figure 3.8. University contributions are steadily increasing. The contributions from industry and government

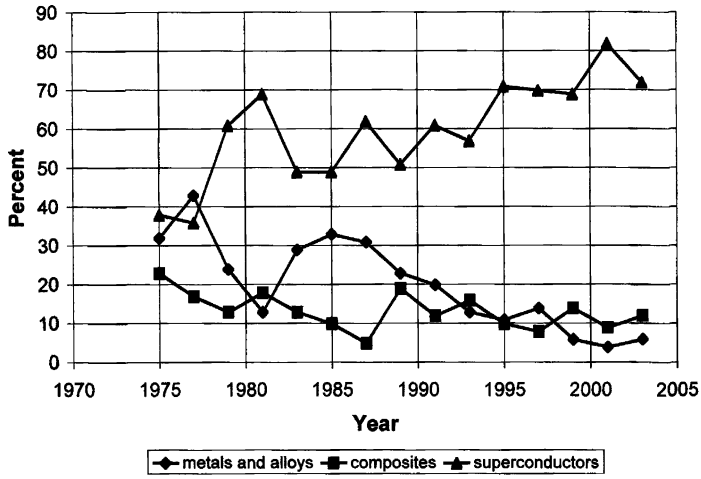

FIGURE 3.7. Topical distribution of US ICMC papers from 1975 to 2003.

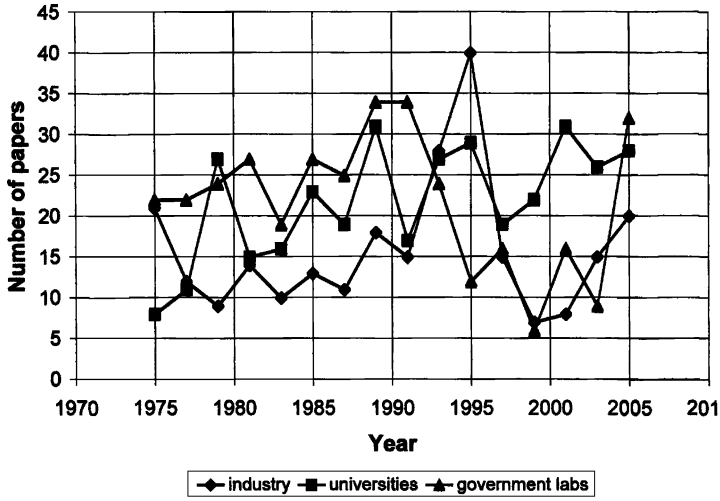

FIGURE 3.8. Distribution of US ICMC papers from companies, industry, and universities.

laboratories are irregular but approximately equivalent and tend to remain constant over time.

The contributions from various US government departments and agencies are plotted in Figure 3.9. The general decline in contributions from the Department of Commerce (exclusively, the National Institute of Standards and Technology

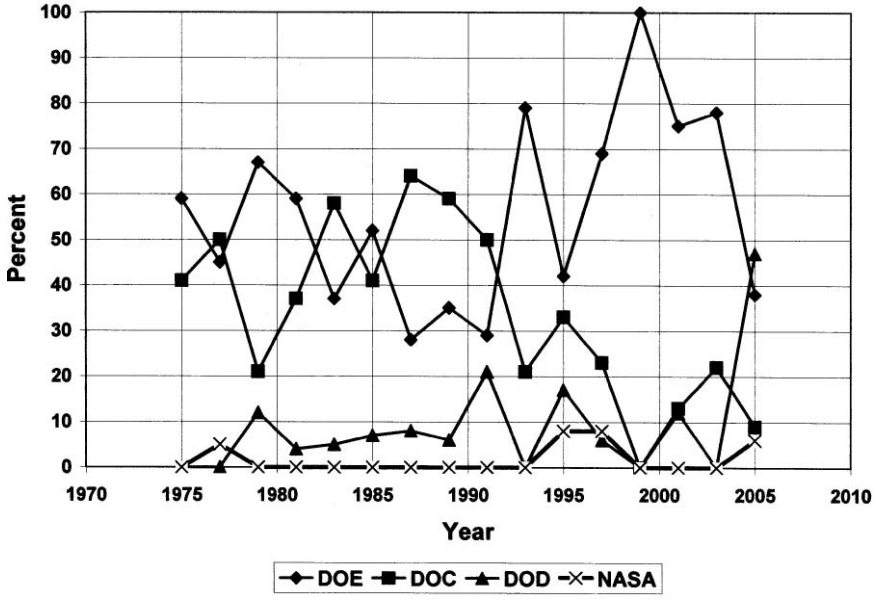

FIGURE 3.9. Percentage of US papers from various US government laboratories.

(NIST)) over the 30-year time frame is due to the gradual reallocation of internal resources to other R&D activities and to abatement of obligations to other agencies. The contributions from research at the Department of Energy (DOE) laboratories (Brookhaven, Argonne, Lawrence Livermore and Berkeley, Fermi, and Los Alamos) have remained at about a constant percentage over time and have usually exceeded those from other government laboratories. Contributions from Department of Defense (DOD) groups have been relatively low but constant until 2005, when a large increase occurred. One wonders whether this portends an adjustment towards low-temperature materials research in several DOD laboratories or whether it represents a reaction toward the first ICMC chairman from a DOD laboratory. Finally, one must be surprised at the very low, particularly in the 14-year time frame from 1979 to 1993, nonexistent contributions from NASA. At best, it contributed only two papers in 1997. The absence of NASA papers clearly suggests a divergent management philosophy, one that forsakes in-house expertise and, thus, sacrifices decision-making and corporate memory relative to materials design, properties, and processing for its emphasis on contracting to many and divergent companies. It is worth noting that very few NASA subcontract results have been reported at ICMC and that, typically, NASA has not sponsored alternative low-temperature material workshops.

In summary, the following trends on low-temperature materials R&D over the past 30 years can be discerned from the papers published in the ICMC proceedings:

- Overall, the total amount of research has increased.
- This increase has been confined to the study of superconductors, whereas R&D on structural metals and alloys, composites and insulators, and functional materials has remained approximately constant.
- Asia's R&D on low-temperature materials has increased notably; that of the US and Europe has increased very modestly.
  - Research on structural metals and alloys has increased in Asia and decreased in the US, relatively.
  - Research on composites (structural composites, resins, electrical and thermal insulation) has declined in the US, relatively.
  - Research on superconductors has significantly increased in all geographic sectors.
- US research on superconductors has increased, relatively, while research on structural metals and alloys and composites has declined.
- US research has been presented in nearly equal numbers by companies, universities, and government laboratories.
- The DOE, of all the US government departments and agencies, has tended to contribute the greatest number of papers, while NASA's contribution has been very low or nonexistent.

3.3 Advances in Cryogenic Materials R&D

This part focuses on advances in low-temperature materials research related to metals and alloys and composites. The application of fracture mechanics and

the related testing to establish sound fracture control for large-scale cryogenic applications are also included. Research on superconductors is not emphasized in this review; others are reporting on this topic.

3.3.1 Fracture Mechanics

During the past several decades, one of the major advances in materials research for cryogenic applications has been the introduction of fracture mechanics concepts, testing, and analysis. In particular, the testing laboratories at the NIST in Boulder, Colorado (Tobler, Read, Reed), at Forchungszentrum Karlsruhe in Karlsruhe, Germany (Nyilas), at the National Institute for Materials Science in Tsukuba, Japan (Ogata), and at the Japan Atomic Energy Research Institute in Naka, Japan (Nakajima, Yoshida, Shimamoto), have been leaders in providing properties and analyses related to fracture mechanics for the cryogenic community.

Fracture mechanics relates particular material properties to flaw size and operational stresses to produce quantitative predictions. Estimates of minimum flaw size that would result in structural failure, maximum allowable operating static and cyclic stress, and expected operational lifetime can be calculated. This section briefly describes the basis, testing and properties, and prediction techniques that are now used in fracture mechanics analysis for cryogenic structures. Good, generalized descriptions of fracture mechanics concepts and utility are found in presentations by Hertzberg [2] and Dieter [3].

The fracture mechanics approach assumes that flaws exist within the structural material. Regardless of their content or geometry, the flaws are assumed to be cracks. The stress distribution K around the crack can be described, in most cases, by the generalized form

$$K = Y\sigma\sqrt{\pi a}, \tag{3.1}$$

where σ is the applied stress and a is the crack (through-thickness) length or depth and Y is a parameter that depends on crack geometry and specimen type or loading parameters. Here, K is called the stress-intensity factor. Tabular lists of Y parameters for various crack locations and geometries have been developed [4–6]. When the stress intensity at the crack tip reaches a critical value, fracture occurs. This critical value is called the fracture toughness K_c. The fracture toughness is a material property, dependent on metallurgical variables, crack orientation, plastic deformation and temperature. When the plastic deformation at the crack tip is very limited, plain-strain loading conditions are prevalent, and the fracture toughness is a minimum value labeled K_{Ic}. When testing, specimen thickness is maximized in an attempt to achieve plain-strain loading conditions.

One can substitute the fracture toughness K_{Ic} for K, the maximum allowable applied stress; σ_{op} for σ; and the critical flaw size a_c for a in Equation (3.1) and use the equation for quantitative assessment of any of the three major design (σ_{op}), material (K_{Ic}), and inspection (a_c) parameters if the other two are known or assumed.

$$K_{Ic} = Y\sigma_{op}\sqrt{\pi a_c}. \tag{3.2}$$

For example, the critical flaw size a_c that will result in fracture can be calculated if one uses the maximum allowable operating stress and minimum value of fracture toughness. Or, if the minimum fracture toughness and minimum inspectable flaw size are known, the maximum allowable operating stress can be calculated. In some cryogenic applications, the calculated critical flaw size may exceed the wall thickness. In these cases, if the structure contains a cryogen, when the crack size exceeds the wall thickness under fatigue conditions, leakage before breakage will occur. In the transport of cryogens, such as liquefied natural gas (LNG), "leak before break" design criteria may be employed, and sensitive leak detection equipment must be demonstrated to preclude subsequent failure and/or dangerous buildup of inflammable gases. In other cases, such as superconducting conduits that contain liquid helium and are enclosed within a vacuum, conduit wall leakage will be evidenced by loss of vacuum.

Ultrasonic, nondestructive inspection (NDI) is usually used to detect small flaws in cases where their size is critical. Flaw sizes of about 5 to 10% of the plate or wall thickness are usually detectable with calibrated ultrasonic NDI techniques.

Maximum allowable stresses for cryogenic applications with ductile structural alloys are usually one-half to two-thirds of the minimum tensile yield strength or one-half of the tensile ultimate strength at the operating temperature, whichever is lower. In many cases, ASME Structural Codes, Section 8 for Pressure Vessel guidelines [7] are followed. Usually, for annealed alloys, such as 316 and 316LN, two-thirds of the tensile yield strength results in a lower allowable stress. When less ductile structural alloys are used, the design criteria are sometimes lowered from one-half to one-third of the tensile ultimate strength.

3.3.1.1 Fracture Toughness

The fracture toughness is usually measured by using compact tension specimens. This type of specimen contains a sharp, machined notch along one side (see Figure 3.10) that is oriented normal to the direction of the applied load. At the base of this notch, a crack is formed by cyclic loading of the specimen at 77 K for fracture toughness tests at 4 K. Guidelines for compact-tension specimen geometry and dimensional tolerances, precracking conditions, and performance of the test are

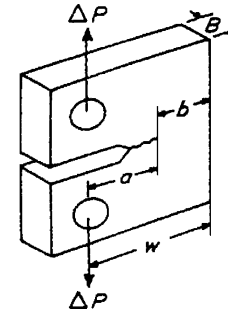

FIGURE 3.10. Compact-tension specimen that is commonly used to measure the fracture toughness and fatigue crack-growth rates, where P is the applied load.

TABLE 3.1. Typical fracture toughness, tensile yield strength, and Young's modulus at 4 K for common structural alloys

Alloy	σ_y(MPa)	K_{Ic}(MPa m$^{1/2}$)	E(GPa)
AISI 304 (annealed)	500	330	209
AISI 316 (annealed)	800	260	207
AISI 316LN (annealed)	1000	215	207
JN-1 (Japan, austenitic)	1240	200	207
Inconel 718 (aged)	1400	110	211
	1200	165	211
Incoloy 908 (aged)	1250	265	175
	1280	155	175
Al 2090-T81	680	50	79
Al 2219-T87	530	45	78
Ti–5Al–2.5Sn (annealed)	1520	35	133
	1291	80	125
Fe–9Ni (quenched, tempered)	1340	70	205
4340 steel (ferritic)	1750	35	200

given in ASTM E-399 [8]. A minimum specimen thickness is always necessary to achieve plane-strain loading conditions. A clip-on strain-gage extensometer that senses crack-opening displacement is usually used to measure crack growth. After precracking, the specimen is loaded at the test temperature to achieve stress intensity levels at the crack tip that are sufficient to promote additional crack growth or immediate fracture. If the specimen fails after limited crack growth and plastic deformation at the crack tip, usually the ATSM guidelines for linear-elastic fracture toughness can be used to calculate the fracture toughness K_{Ic} from the load–crack-growth curve. If more extensive crack growth and associated plastic deformation occur prior to fracture, elastic–plastic conditions are prevalent, and the J-integral ASTM E-813 test guidelines [9] must be employed to measure $K_{Ic}(J)$.

Typical values of the fracture toughness at 4 K for common structural alloys are listed in Table 3.1. The reader is cautioned, however, that for any particular alloy, there can be large variabilities in the fracture toughness at 4 K that result from the amount of cold work, heat treatment, impurity levels, grain size, amount and location of precipitates, and specimen crack orientation relative to the orientation of these metallurgical variables. Owing to this sensitivity of low-temperature fracture toughness on metallurgical parameters, it is necessary to conduct fracture toughness measurements at the lowest operating temperature and to use specimens with cracks oriented in specific worst-case directions on heats of alloys selected for use.

Also included in Table 3.1 are the tensile yield strength σ_y and Young's modulus E for the same metallurgical condition corresponding to the fracture-toughness condition. The tensile yield strength, like fracture toughness, is considerably more sensitive to metallurgical and test variables at 4 K than at room temperature. (For example, see the discussion of the temperature dependence of nitrogen addition and grain size on yield strength of austenite in Section 3.3.2.1.) Therefore, tensile

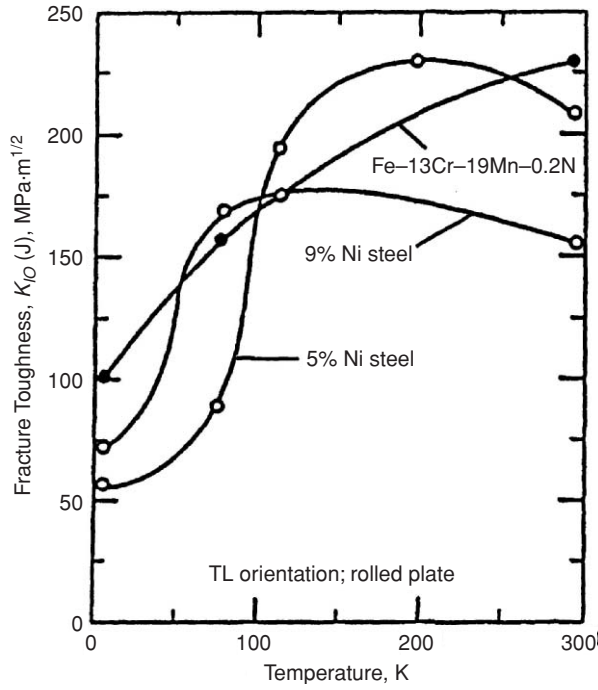

FIGURE 3.11. Fracture toughness of two ferritic steels (Fe–5Ni, Fe–9Ni) and one austenitic steel (Fe–13Cr–19Mn–0.2N) at low temperatures.

tests of actual alloy heats used for fabricating cryogenic devices are required when the design stress levels and design yield strengths are close to each other.

The fracture toughness depends only mildly on temperature for most face-centered cubic metals and alloys (e.g. aluminum and copper alloys, austenitic steels). An example is the temperature dependence of the austenitic Fe–13Cr–19Mn–0.2N steel shown in Figure 3.11. Most body-centered cubic (e.g. ferritic and martensitic steels, refractory metals) and hexagonal close-packed alloys (e.g. titanium and magnesium alloys) exhibit a *ductile-to-brittle transition* at lower temperatures, as illustrated for two ferritic/martensitic Fe–Ni alloys in Figure 3.11. The temperature range of the transition can be lowered by improving alloy purity and, in the case of ferritic/martensitic steels, also by modifying the composition and heat treatment.

3.3.1.2 Fatigue Crack-Growth Rate

By using identical or very similar compact-tension specimens and ASTM E-647 guidelines [10], fatigue crack-growth rates da/dN (where a represents crack growth and N is the number of fatigue cycles) can be measured. In such tests, crack extension is continuously monitored with strain-sensing equipment similar to that used in fracture-toughness testing. Maximum and minimum stresses (ΔK values) are never negative during these tests ($R > 0$). During the test, increasing

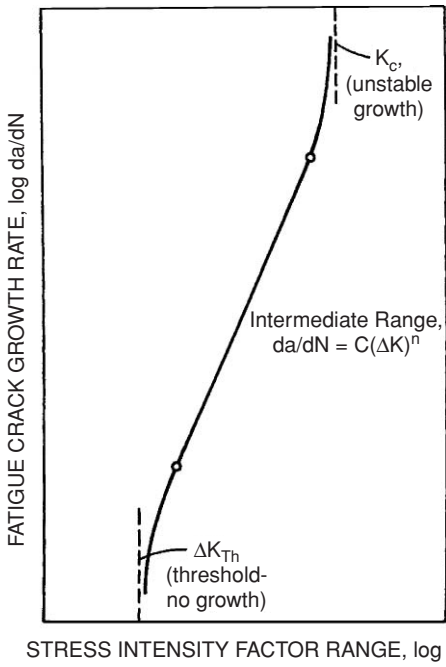

FIGURE 3.12. Schematic curve of fatigue crack-growth rate versus applied K, illustrating the three stages of crack-growth rates.

crack extension results in ever-increasing stress intensity at the crack tip; thus, one obtains crack-growth rates as a function of ΔK during each test.

Plots of log da/dN versus log ΔK have three stages, as depicted in Figure 3.12. At low ΔK and da/dN levels, a ΔK threshold value is reached, below which there is no detectable crack growth during fatigue cycling. At intermediate values of each variable is the *Paris range*, where log da/dN is linear with log ΔK and

$$\mathrm{d}a/\mathrm{d}N = C(\Delta K)^n. \tag{3.3}$$

Here, C and n are constants that vary with alloy and test parameters (such as R, the ratio of $\Delta K_{\max}$ to $\Delta K_{\min}$). At higher ΔK values, crack growth is accelerated and ΔK approaches the fracture toughness K_c. These concepts are illustrated in Figure 3.12.

Fatigue crack-growth rates at 4 K of a number of structural alloys are presented in Figure 3.13. Note that the very brittle (at 4 K) Fe–9Ni alloy has much higher fatigue crack-growth rates than the other structural alloys. In Figure 3.13, the "normalized" values of $\Delta K/E$, plotted versus da/dN, are also included. Similar to the case of K_{Ic}/E versus σ, plotting 4 K data in this manner results in much smaller variability for a large range of different structural alloys. The da/dN is virtually independent of temperature (over the range 4 to 300 K) for austenitic steels (see Figure 3.14 for the temperature dependence of 316LN); this is likely true for most face-centered cubic metals and alloys.

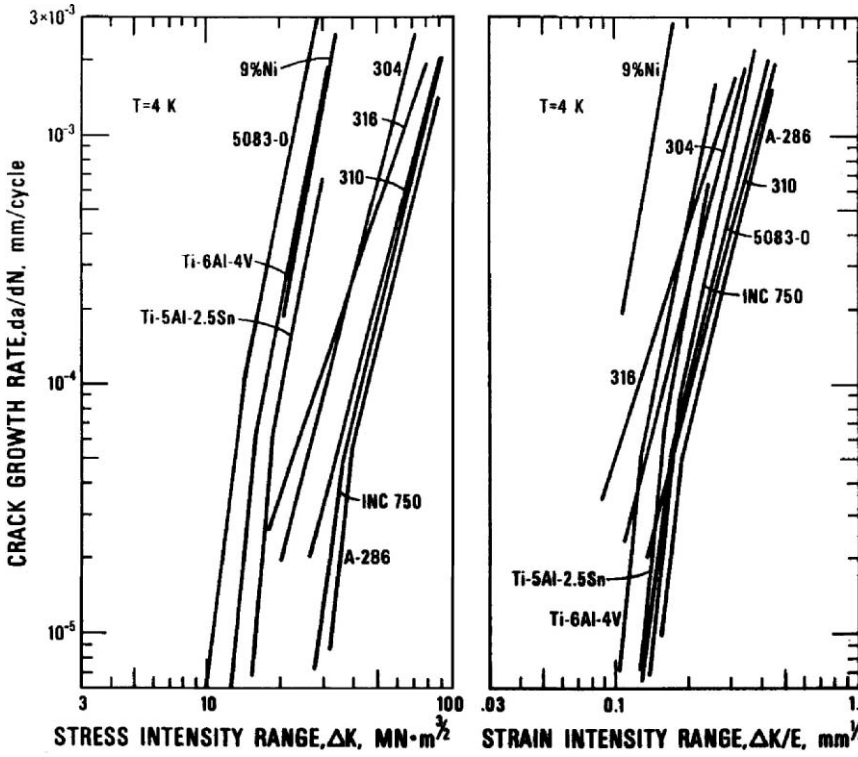

FIGURE 3.13. Fatigue crack-growth rates for austenitic steels (304, 316, 310, A-286), titanium alloys, an aluminum alloy (5083-0), an age-hardened nickel alloy (INC 750), and a ferritic steel (9% Ni) as a function of applied ΔK and "normalized" $\Delta K/E$.

Equation (3.3) is used to estimate the length of crack growth with prior knowledge of the initial stress intensity (from crack configuration and cyclic applied stress), initial flaw size (from NDI), and desired operating lifetime. Typically, estimates of the initial flaw size are derived from estimates of the minimum measurable size from ultrasonic inspection. Flaws may safely grow under fatigue conditions (subcritical crack growth) until the critical flaw size (determined from fracture toughness tests and described earlier) is reached; at that time catastrophic failure will occur. Safety factors of at least two are employed in the design criteria to account for measurement imprecision and material variability.

3.3.2 Austenitic Steel Advancements

Austenitic steels have been selected almost exclusively as the structural material for restraining the magnetic forces of superconducting magnets. Their excellent toughness and relatively high strength, combined with high elastic modulus, low

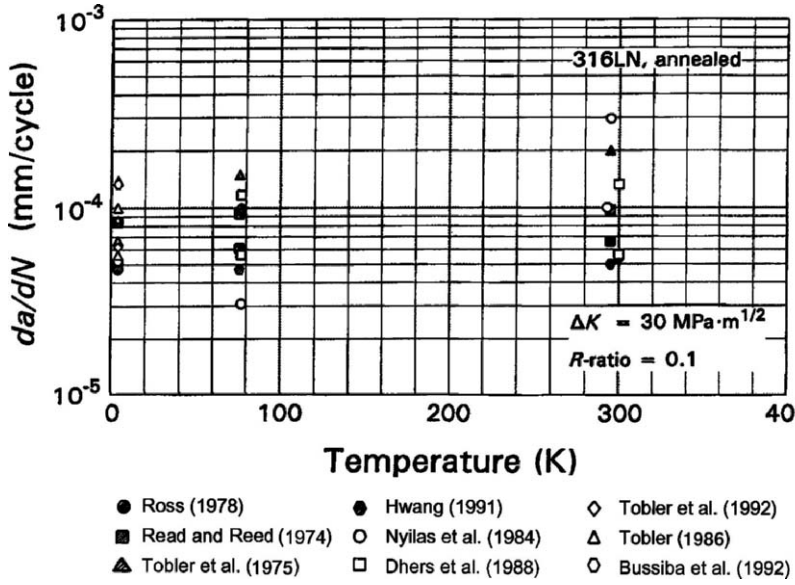

FIGURE 3.14. A compilation of the measured temperature dependence of da/dN for austenitic steel AISI 316LN at a constant ΔK of 30 MPa m$^{1/2}$ and R ratio of 0.1.

magnetic permeability, low thermal and electrical conductivities, and relative ease of welding, have led to their selection for many cryogenic applications. On the basis of the emphasis placed on the use of austenitic steels for the principal structural alloy for the case and, perhaps conduit, for the International Thermonuclear Experimental Reactor (ITER), a tremendous amount of research on this alloy class has been conducted over the past 20 years. This effort includes development of an entirely new set of commercial-grade, high-nitrogen austenitic steels in Japan. Development of these steels followed realization, through research in the US (NIST: Tobler, Read, Reed, Simon, Walsh) and Japan (Japanese Atomic Energy Research Institute (JAERI): Shimamoto, Yoshida, Nakajima; Nippon; Kobe; Japanese Steel Works; and Kawasaki steel companies) that adding nitrogen, relatively inexpensively, to base-300-series stainless steels resulted in substantial increases of the tensile yield strength at 4 K. Primarily strength, toughness, and fatigue mechanical properties and contraction and conductivity thermal properties have been measured. The effects of thickness, orientation with respect to the rolling direction, metallurgical and processing variables, and test parameters have been studied on this alloy class for 4 K applications. This section briefly reviews selected advances from this research over a number of decades under the subsections of strength, toughness, and alloy development. Over this period of time, a number of reviews that include development, low-temperature properties, welding, and utilization of austenitic steels for cryogenic applications have been published [20–30].

3.3.2.1 Strength

Although it has been known for a long time that nitrogen additions to austenitic steels increases their strength, only in the past 20 years has nitrogen strengthening been used to develop alloys for use at cryogenic temperatures [20]. The addition of nitrogen to the melt of austenitic steels through alloying (such as adding chrome nitride) or through gas (bubbling under positive pressure) is relatively easy and not expensive. The addition of nitrogen increases austenite phase stability, corrosion resistance, and improves strength. Nitrogen occupies interstitial lattice sites in the austenite matrix, and it is especially effective in increasing strength at low temperatures. The temperature dependence of the nitrogen-strengthening effect is quite strong: The addition of 0.1 wt% nitrogen increases the σ_y at room temperature by about 50 MPa, but the same amount of added nitrogen results in an increase in σ_y of about 250 MPa at 4 K—a factor of five difference. Figure 3.15 depicts the dependence of σ_y on nitrogen as a function of temperature [20]. The

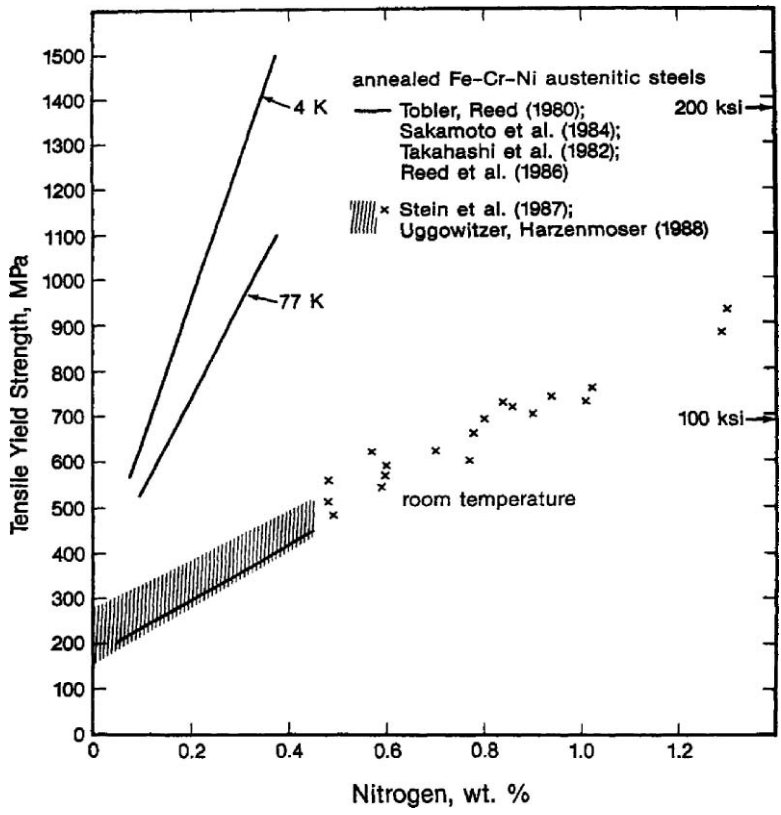

FIGURE 3.15. Dependence of the tensile yield strength on nitrogen content for Fe–Cr–Ni austenitic steels at 295 K, 77 K, and 4 K [31–36].

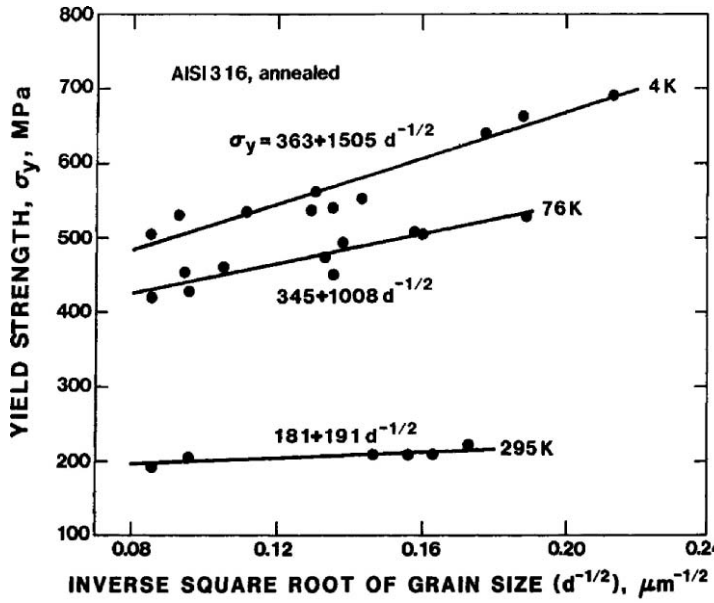

FIGURE 3.16. Dependence of tensile yield strength on grain size in annealed AISI 316 austenitic steel as a function of temperature.

alloys with nitrogen contents above about 0.5 wt% were produced by using special, noncommercial, pressurized nitrogen atmospheres with electroslag-remelting techniques.

The yield strength of an austenitic steel also depends on its grain size. Figure 3.16 illustrates that smaller grain sizes result in stronger alloys and also indicates that this strengthening effect is temperature dependent. At 4 K the dependence of σ_y on grain size is approximately twice that at room temperature. Indeed, grain size variability from 50 to 100 μm in an austenitic steel plate results in variations of σ_y of ±100 MPa. In Figure 3.16, a Hall–Petch relationship is assumed: $\sigma_y = kd^{-1/2}$, where d is the average grain diameter and k is a constant.

The yield strength at 4 K is predictable for AISI 316-type austenitic steels if one uses a linear fit for dependence on [N] content (weight percent) and a Hall–Petch fit ($d^{-1/2}$, where d is in micrometers) for the grain size dependence:

$$\sigma_y(\text{MPa}) = 430 + 2500[\text{N}] + 740\ d^{-1/2}. \tag{3.4}$$

This relationship was obtained from regression analysis of about 100 NIST tensile measurements at 4 K of AISI 316, 316LN, and 316LHN alloys produced in the US, Japan, and Europe [21]. The standard deviation of the fit to the data is 45 MPa, and the standard deviations of the three coefficients are 20 MPa, 90 MPa, and 116 MPa respectively. The use of Equation (3.4), or similar equations developed for other austenitic steels, enables alloy design to a preselected tensile yield

strength by either variation of the nitrogen content or thermomechanical processing to affect the grain size.

The addition of carbon is not as effective as the addition of nitrogen in increasing austenitic steel strength at 4 K. The contribution from carbon is about half that of nitrogen for equivalent weight percent additions. Additionally, carbon additions decrease the weldability of austenitic steels and increase the tendency toward sensitization (embrittling carbide forms at grain boundaries during cooling through the temperature range from about 300 to 600 °C after welding).

The additions of solid-solution alloying elements, such as molybdenum and manganese, contribute to strength increases at 4 K much less significantly, and properties resulting from these additions have not been clearly characterized. Cold work also increases low-temperature strength, but, again, data are insufficient to provide quantitative detail.

3.3.2.2 Toughness

At low temperatures, the toughness of austenitic steels depends strongly on their strength, nickel content, impurity level, and inclusion spacing.

At NIST, extensive testing of various commercial grades of austenitic steels at 4 K established a clearly linear relationship between decreasing fracture toughness and increasing tensile yield strength (see Figure 3.17). All the strengthening mechanisms described in the previous section contribute to reductions of austenitic steel toughness. Throughout the yield strength range of about 300 MPa to 1500 MPa, the fracture toughness (both linear elastic and J-integral) was found to decrease linearly in 4 K tests from about 350 $MPam^{1/2}$ to 50 MPa $m^{1/2}$ respectively.

The addition of nickel beyond the 8 wt% normally required for most specifications of austenitic steels increases the low-temperature toughness of these steels, as illustrated in Figure 3.18 for an Fe–20Cr–4Mn base alloy with sufficient nickel additions to ensure austenite stability. Nickel additions also increase the stacking-fault energy. Thus, in alloys of higher nickel content, one expects less deformation-induced martensitic transformation products (from increased nickel stability and stacking-fault energy) and less deformation twinning (from increased stacking-fault energy).

Cracks initiate primarily at inclusion sites in ductile austenitic alloys. Alloys that contain fewer or smaller inclusions, usually referred to as *cleaner steels*, exhibit higher toughness at low temperatures. The reduction of impurity content contributes to cleaner steels. A number of mills, at added cost, can process austenitic steels by using electroslag remelting (ESR); this process results in considerably cleaner steels. Current specialized melting practices, such as ESR, result in phosphorus and sulfur levels below about 0.015 wt% and 0.005 wt%, respectively, which is a significant improvement over conventional practices that result in weight % ranges of 0.020 to 0.045 for these impurities. Quantitative correlations between increasing inclusion content and decreasing fracture toughness have been

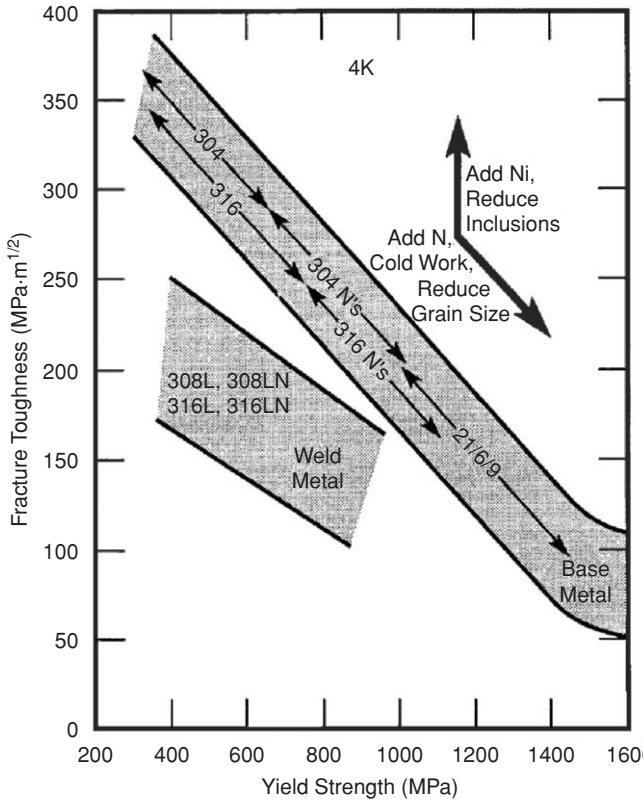

FIGURE 3.17. Trends of the dependence of fracture toughness on tensile yield strength at 4 K of austenitic steels as influenced by variations of cold work, grain size, nickel content, inclusions, and welding.

determined for austenitic steel welds. Estimates for 316LN base metals at 4 K were determined by the ITER project [29]:

$\sigma_y = 1080$ MPa	inclusion spacing $= 0.06$ mm	$K_{Ic} = 160$ MPa m$^{1/2}$
$\sigma = 1080$ MPa	inclusion spacing $= 0.14$ mm	$K_{Ic} = 350$ MPa m$^{1/2}$
$\sigma = 930$ MPa	inclusion spacing $= 0.06$ mm	$K_{Ic} = 210$ MPa m$^{1/2}$
$\sigma_y = 930$ MPa	inclusion spacing $= 0.14$ mm	$K_{Ic} = 400$ MPa m$^{1/2}$

Inclusion spacings larger than 0.14 mm are found in high-purity ESR-treated material. Weld-metal inclusion spacings are typically less than 0.10 mm.

In Figure 3.17, note that the fracture toughness of stainless steel welds is lower than that of the base metals at 4 K for equivalent yield strength. Usually this difference is due to the larger size and amount of inclusions within the welds, although, in some cases, ferrite is present, and premature cracking in this phase leads to degradation of weld toughness.

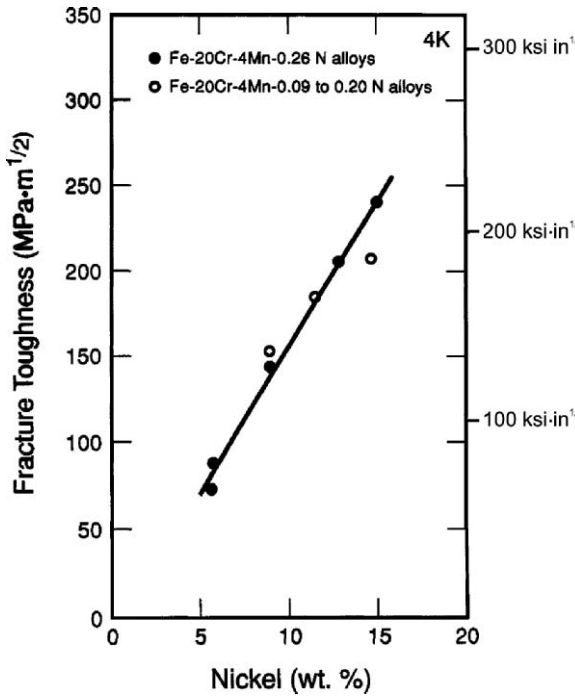

FIGURE 3.18. Dependence of fracture toughness at 4 K for two austenitic steels as a function of nickel content.

3.3.2.3 Alloy Development

A number of improved austenitic steel alloys were developed in Japan during the early 1980s. At that time, the JAERI encouraged the Japanese steel companies to develop extremely strong and tough austenitic steels by establishing design objectives for structural alloys to be used in high-field superconducting magnets of the ITER project [30]. After taking into consideration high magnetic forces and the ability to inspect austenitic steels and then adopting fracture mechanics principles to establish a sound fracture control plan, JAERI arrived at the alloy research objectives of 200 MPa $m^{1/2}$ fracture toughness and 1200 MPa tensile yield strength at 4 K. Since construction of these objectives produces two sides of a box on toughness–yield strength plots (see Figure 3.17), these guidelines were termed the *JAERI box*. As Figure 3.17 shows, these guidelines were considerably above the tensile and toughness properties of commercial-grade steels at the beginning of the 1980s. The Japanese steel industry (Nippon, Kobe, Kawasaki, Japanese Steel Works) chose to use both Fe–Cr–Ni and Fe–Cr–Mn alloys to develop six or seven new austenitic steels whose strength and toughness at 4 K were sufficient to be placed within the JAERI box. Better manufacturing practices (vacuum-induction melting, ESR, vacuum oxygen decarburization, submerged-arc refining, rapid cooling after hot rolling), use of higher purity alloying (e.g. electrolytic-grade manganese) and alloy additions (nickel and, in some cases, chromium) to improve

toughness; nitrogen to improve strength; and manganese and chromium to increase the nitrogen solubility range) were employed. Impurities were maintained at very low levels: less than 0.005 wt% sulfur, usually less than 0.015 wt% phosphorus, and minimal oxygen. Use of large-capacity hot-rolling mills led to smaller, more uniform grain sizes. This consistently small grain size, combined with hot work, also improved the yield strength of these alloys at 4 K.

3.3.3 Nonmetallic Composite Electrical Insulation

Considerable improvements and characterization of existing nonmetallic composites and development of new composites for use as electrical insulation at low temperatures have taken place over the last few decades. In particular, glass-fiber-reinforced epoxy-resin matrix composites have been rather thoroughly studied. Applications have focused primarily on turn, layer, and ground insulation and on matrix bonding of superconducting coils. Many have made strong contributions: Okada and Nishijima (Osaka University) in Japan; Evans (Rutherford Laboratories) and Broadbent (Oxford Instruments) in England; Rey (CEA/Saclay) in France; Weber (Atominstitut der Österreichischen Universitäten) in Austria; and Kasen, Schramm, and Simon (NIST), Fabian, Munshi, Rice, and Schutz (Composite Technology Development, Inc.), Benzinger (Spaulding Fiber, Inc.), and Reed (Cryogenic Materials, Inc.) in the US.

Other research on composites has been directed toward low-temperature, thermal–mechanical support structures, such as straps and struts (tubes, cylinders). Adequate reviews of developments and properties for thermal–mechanical supports have been presented previously [37,38]. This presentation is limited to applications for superconducting coils.

Three general types of composites are prepared by different fabrication schemes for use as electrical insulation of superconducting coils. The fabrication techniques are high-pressure lamination (HPL), resin preimpregnation (usually called *prepreg* (PP)), and resin-transfer molding (commonly called *vacuum-pressure impregnation* (VPI) by the superconducting-coil community). Properties and characteristics of composites fabricated by these three techniques are compared in Table 3.2. Recent advances in each of these areas are presented in the following subsections. Advances in the development of new resins, in new test techniques, and in radiation testing and analysis are also discussed.

3.3.3.1 High-Pressure Laminates

For many years, the composite laminates used in plate or block form in superconducting coils for fill within spaces, as buffer zones, to brace incoming or outward going leads, and for ground or layer insulation have been the National Electrical Manufacturers Association (NEMA) grades G-10 and G-11. These grades are composed of E-glass fibers and bonded within a matrix of epoxy resin. However, as the sophistication of superconducting coil design increased, so did the need to know more precise mechanical, thermal, and electrical properties at the operating

TABLE 3.2. Typical properties at 4 K and characteristics of glass–epoxy composites used in superconducting coils (50 vol.% glass content)

	Type of composite		
Property	HPL (G-10CR)	PP (TGDM–glass–Kapton)	VPI (epoxy–glass)
Density (g/cm^3)	1.8	1.8	1.8
Young's modulus (GPa)			
in plane	35	22	22
through thickness	22		
Shear modulus (GPa)			
interlaminar	9.0	4.4	7.6
Shear strength (MPa)			
interlaminar	80	40	70
Compressive strength (MPa)			
through thickness	800	800	800
Thermal contraction 295 K $\rightarrow$ 4 K (%)			
in plane	0.24	0.20	0.20
through thickness	0.72	0.70	0.73
Thermal conductivity [W/(m K)]			
through thickness (4 K/300 K)	0.030/0.55	0.064/0.47	0.062/0.50
Inspection	Complete visual	Complete visual	No visual
	Detailed electrical	Detailed electrical	General electrical
Repair	Complete exchange of parts	Defect cut/grind followed by replacement PP	Not possible
Manufacture	Independent of coil fabrication	Wrap around conduit/conductor	On line
	Industrial laminate	Off line	Final stage
		Under pressure, cure at 150–300 °C	Complete coil resin cure at 110–150 °C

temperature of 4 K. It was discovered that the NEMA specifications for G-10 and G-11 were astoundingly broad. Various types of E-glass cloth weaves could be used; the volume fraction of glass varied more than 25%; many different resin systems could be used with or without fillers (SiO_2, Al_2O_3); the pressure and temperatures for the high-pressure laminate cure were not specified; and the maximum porosity was not specified. Whereas these broad specifications, primarily electrical, had been sufficient for most uses at room temperature, they resulted in very large property variations at cryogenic temperatures. With this incentive, Kasen (NIST), working primarily with Benzinger (Spaulding) and the NEMA committees, was successful in developing two specialized grades of high-pressure laminates that had much narrower specifications: NEMA grades G-10CR and G-11CR. They were developed in the late 1970s, and their low-temperature mechanical, thermal, and electrical properties were thoroughly characterized [39,40].

The NEMA grades G10-CR and G11-CR are produced under high pressure (about 7 MPa). Consequently, their void content is very low and their glass content is relatively high (55 to 65 vol.%). Thus, their mechanical and electrical properties tend to be quite good. The laminate grades can be procured in various shapes (plates and cylinders) and sizes (as thick as 10 cm), and other forms can be obtained by cutting and/or grinding. Recently, however, it has not been possible to obtain G11-CR in other than complete mill runs, owing to lack of demand for this grade.

3.3.3.2 Pre-impregnation

The use of pre-impregnation of glass cloth with resin that assumes a very viscous, sticky (B-stage) composure, called *prepreg*, had limited use for the insulation of superconducting coils. However, for the ITER central solenoid model coils (one each was constructed in the US and in Japan) in which the react, then wind coil-fabrication sequence was employed, the turn insulation around the conduit was fabricated by using composite prepreg technology [41]. With this procedure after the Nb_3Sn reaction, the pre-impregnated cloth in tape form is cowound with Kapton tape around the conduit. It is then cured and inspected prior to winding the insulated conduit onto the coil mandrel. The resin-cure cycle is performed under pressure (expandable silicone rubber sleeves may be used) at slightly elevated temperatures (about 150 to 300 °C). Advantages of this fabrication technique include: (1) use of Kapton film for an electrical barrier that does not impede the flow or placement of resin is an option; (2) complete visual and electrical inspection is possible; (3) repair procedures are relatively easy and not space restricted if local areas of the prepreg composite sheath do not meet the inspection criteria; (4) more radiation-resistant resin systems than the low-viscosity resins required for the VPI process can be used when needed; (5) the pressure cure ensures a better bond between the turn insulation and conduit; and (6) the pressure cure in combination with the independent strength and orientation of each turn of the precured prepreg composite (with or without Kapton) acts to preclude failure of the turn insulation system and to limit debonding from the conduit when tensile forces are generated between the turn insulation and conduit of the coil during cool-down or operation. Balanced against these many positive factors are the relative novelty of this process in the superconducting coil community, the costs that are added to procure special orders of prepreg tape, and the time and costs for setup and pressure-curing at elevated temperatures of the prepreg resin system after winding around the conduit. Also, the use of epoxy-based prepreg turn insulation precludes the wind-and-react fabrication coil procedure.

3.3.3.3 Resin-Transfer Molding (Vacuum-Pressure Impregnation)

The last step in the fabrication of superconducting coils is the transfer of resin into the coil form to bond all turns into a monolithic structure. The three, fundamentally different approaches to this resin-transfer process are (1) flood filling, (2) partially sealed tool, and (3) sealed tool. In the flood-filling technique, the coil is placed within a containment vessel, and this system is placed within a vacuum chamber. After evacuation, resin is pumped or poured into the containment vessel. This

most simple system has been used for some of the coils in the CERN Atlas program and in increasing applications of magnetic resonance imaging (MRI), where routine coil fabrication of many similar coils is required. In the partially sealed tool technique, the coil is placed within a resin-tight (but not vacuum-tight) tool assembly that is then positioned in a vacuum chamber. Resin is transferred into the tool assembly after evacuation. The sealed-tool technique consists of vacuum- and resin-tight tooling surrounding the coil. Resin is transferred into the tooling following evacuation. Traditionally, this technique has been used on one-of-a-kind coils and on most large-scale coils.

A detailed report [42] of the very large-scale VPI process for the US ITER central solenoid model coil (about 2.7 m in diameter and about 2.84 m high) includes resin data, laboratory resin-flow research and trial runs, resin-injection equipment, large-scale trial runs, model-coil tooling and temperature and pressure control, and input data during the transfer of 1400 L (370 gal) of resin into the coil. To assist resin flow for the VPI process and to provide strength, glass-cloth tape is wound around each conduit or conductor prior to assembly into coil form. The resin plus glass cloth form a glass–epoxy composite whose strength depends on the volume fraction of glass, the amount of porosity within the cured resin, temperature, radiation, and orientation of the applied stress relative to the orientation of the glass-cloth layers. Interlaminar shear strengths (with cracks running only through the matrix resin) are always lower than in-plane tensile or compressive strengths. During the past 20 years, the effects of many of the variables listed above on the orientation-dependent strengths of glass–epoxy composites have been investigated. The influence of radiation (so important for potential superconducting magnets for fusion and high-energy physics) on VPI composite mechanical properties at low temperatures has been examined. In most superconducting coils that are exposed to large radiation doses (especially neutron), the glass–epoxy composite formed by the VPI process has been considered the weak mechanical link in the complex superconducting coil structure.

Unfortunately, use of the VPI-produced composite structure as an integral electrical insulation system presents problems:

- The setup and process is time consuming, expensive, and very detailed to prevent vacuum and resin leaks and to ensure complete resin flow throughout the coil.
- The resulting glass–epoxy composite insulation cannot be inspected, and internal defects are not repairable.

During the resin impregnation process, the flow of the resin throughout the entire coil, usually from the resin inlet at the coil bottom to the outlet(s) at the top of the coil, may be irregular and follow the path of least resistance. This may result in areas void of resin within the coil. Sometimes, these voids cannot be seen from the surface of the coil. Even if they are observed, they are seen only after resin cure and removal of the coil tooling. Thus, the builder is faced with the dreaded decision of either accepting the flawed coil or starting the fabrication process all over again. Intuitively, design of one-of-a-kind, noncommercial coils should strive for the independent mechanical and electrical integrity of the turn, layer, and ground insulation through the use of high-pressure laminates and prepreg composites.

3.3.3.4 Test Techniques

Glass fibers act to both stiffen and strengthen glass–resin composites. They stiffen because their elastic moduli are considerably higher than the resin. They strengthen because the fibers act as crack arrestors: cracks prefer to grow through the resin matrix, not through layers of glass cloth. Thus, crack propagation under interlaminar shear always is rather easy, as there are no glass layers along this path to impede crack growth. This results in relatively low values of the interlaminar shear strength. However, the interlaminar shear strength depends on the associated normal stress, whether that be in compression or tension. In superconducting coils, cool-down and magnetic forces produce both interlaminar shear and, usually, normal compressive forces on the glass plies of the turn insulation. A new test was developed to measure the "shear/compression" strength of composites [43]. This test enables variation of the ratio of applied interlaminar shear to normal compressive stresses on composite or bonded specimens at any desired temperature (see Figure 3.19 for specimen and loading details). A plot of shear/compression properties for a VPI E-glass cloth–epoxy composite is shown in Figure 3.20. Fatigue tests can also be conveniently conducted with this measurement procedure. In Figure 3.20 note that the fatigue strengths at $10^5$and 10^6 cycles at 76 K are included. From the figure, static and fatigue strengths can be easily compared and design envelopes with appropriate safety factors obtained.

This shear/compression test has been used during the past 15 years to quantify the applicable properties of various proposed insulation systems and to assess the radiation sensitivity of resin systems. They may also be used to provide quantitative design criteria to establish maximum allowable shear/compression operation stress levels.

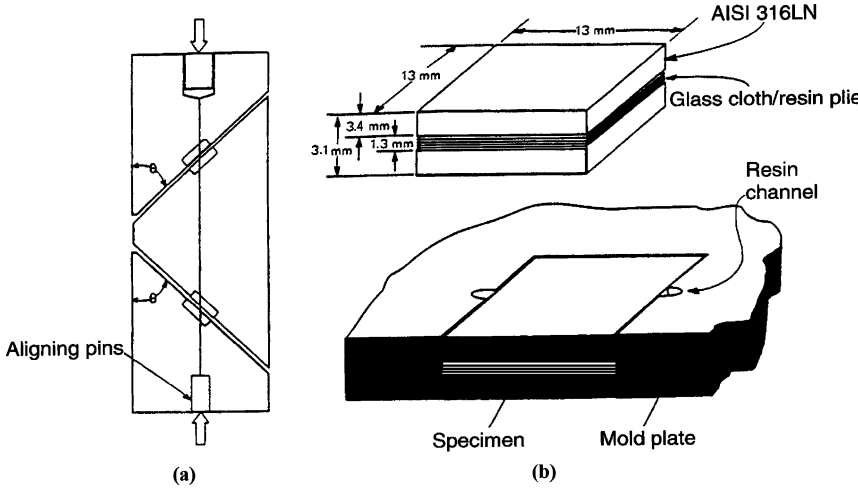

FIGURE 3.19. (a) Schematic of test fixture and specimens used to load two composite insulation specimens in shear and compression. (b) Specimen configuration (later specimens were circular in shape) and mold used to fabricate specimens using either the VPI or PP process.

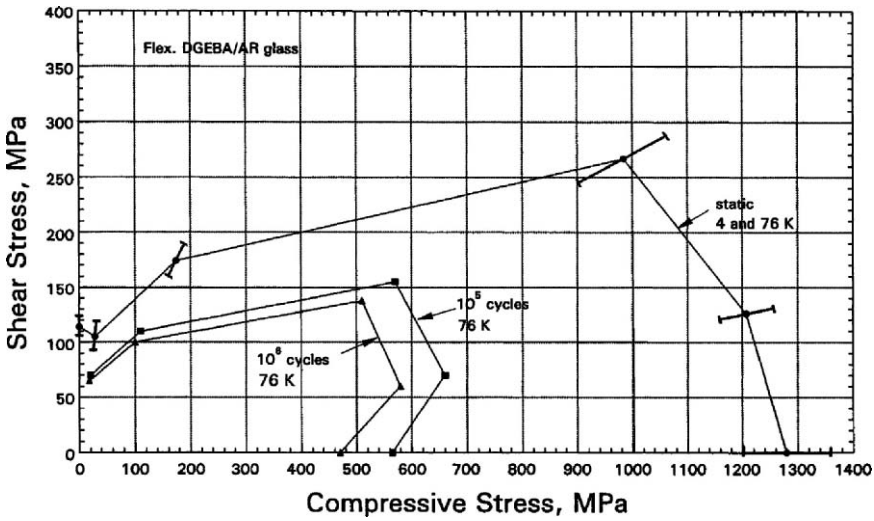

FIGURE 3.20. Combined shear and compressive stress to cause failure of VPI fabricated epoxy as-received (AR) S-glass specimens with about 50 vol.% glass under static loading (4 K and 76 K) and after 10^5 and 10^6 fatigue cycles at 76 K for various loading angles (ratio of shear to compressive stress).

During this time period, the dramatically increased computer capabilities have led to more precise and comprehensive finite-element stress analyses for superconducting coil insulation systems. These analyses have been assisted by measurements of some of the nine elastic constants for the orthotropic fiber-reinforced composites. Unlike isotropic metals, along the three major axes of fiber-reinforced composites (warp, fill, through-thickness for glass-cloth reinforcement), both tensile/compression and shear elastic constants and the associated Poisson's ratio are all distinct. Even now, additional ultrasonic or resonance measurements at low temperatures could increase the accuracy of these constants and indicate their variability with glass content and processing pressure. However, the inclusion of detailed stress analyses combined with improved compression and shear-strength measurement techniques has led to the inclusion of mechanical properties in the design criteria for composite electrical insulation for large superconducting coil projects.

3.3.3.5 Radiation: Resins and Coatings

Most applications for superconducting coils in the recent past have been for MRI medical equipment; large, high-energy physics facilities; and fusion plasma containment (ITER). In the latter two applications, coils must operate in a radiation environment. Nonmetallic composite matrix resins are usually the most radiation-sensitive component within these coils. Consequently, there have been a number of studies to characterize the more sensitive mechanical properties at 4 K to radiation dose or neutron fluence. Associated with these studies has been the introduction of new resin and insulation systems that are more radiation resistant. Leaders in

the development of these potentially better systems have been Evans, formerly of Rutherford–Appleton Laboratories in England, Composite Technology Development, Inc. in the US, and Nishijima and Okada of Osaka University in Japan (JA).

Some of the resin systems that have recently been used in large-scale magnets projects are[1]

DBEBA/anhydride epoxy	CERN Atlas	VPI
	JA (central solenoid coil)	VPI
	EU (toroidal field coil)	VPI
DGEBF–anhydride	US (central solenoid coil)	VPI
DGEBF–DETD–PPGDGE	CERN Atlas	VPI
TGDM–aromatic amine	US (central solenoid coil)	PP (turn insulation)

Other systems have been developed and proposed for use in superconducting coils that are exposed to very large radiation doses (>5×10^7 Gy) [44–48]:

cyanate ester	VPI
cyanate ester–polyimide	VPI, HPL
cyanate ester–epoxy	VPI, HPL
ceramic	PP, coating
ceramic–epoxy	VPI

The cyanate ester systems are more radiation resistant than the epoxy systems listed earlier, but, unfortunately, they are quite a bit more expensive. Cyanate ester–epoxy or polyimide blends have been proposed to reduce the added costs somewhat. Utilization of ceramic prepreg or coating, wound around or applied to the conductor, enables the use of the wind, then react, coil-fabrication procedure. The ceramic prepreg, after curing to a green state at around 150 °C, will solidify and withstand the Nb_3Sn reaction heat treatment of 600 to 700 °C for about 240 h. Research has also been directed toward application of a ceramic coating directly on the conductor and to anodization, if the conductor is aluminum; both of these possibilities enable the use of the wind, then react, coil-fabrication sequence.

After radiation at low temperatures and warming to room temperature H_2, CO, and CO_2 gases are formed in epoxy resin systems. Some of the gas molecules diffuse and escape from the composite surface, especially the smaller H_2 molecules. Typical gas evolution rates of about 1.2 $cm^3/g \cdot MGy$ have been measured for epoxy resin systems; the evolved gas is primarily hydrogen [49]. This evolved hydrogen gas must be considered a safety issue during coil warm-up.

Some of the gases, mostly the larger CO and CO_2 molecules that have more trouble diffusing through the matrix, remain trapped within the composite and contribute to internal swelling. Swelling as much as 5 to 6% in the through-thickness direction of glass–epoxy composites has been reported for dose levels of 5×10^7 Gy [50]. Similar measurements along in-plane directions revealed no

[1] DBEBA: diglycidyl ether of bisphenol-A; DGEBF: diglycidyl ether of bisphenol-F; DETD: diethyl toluene diamine; PPGDGE: polypropylene glycol diglycidyl ether; TGDM: tetraglycidyl diaminodiphenyl methane.

evidence of swelling. Quite obviously, the presence of swelling would contribute to increased compressive stress in the through-thickness direction of the insulation systems.

When conducting tests to assess the radiation sensitivity of various matrix resin systems within glass–resin composites, it is very important that the test be designed so that the crack path proceeds within the resin system and does not have to intersect layers of glass cloth, for it is the resin that is sensitive to radiation; glass remains insensitive at radiation levels normally contemplated for use in superconducting coils. Interlaminar shear testing results in crack initiation in the resin system and growth within the resin layers bounded by the laminar glass cloth. All other compression and shear tests result in crack-growth intersection with glass-cloth layers. Many such cryogenic tests have been reported in the literature.

3.3.4 Superconductors

Rapidly following the identification of the presence of high-temperature superconductivity in the Ba–La–Cu–O alloy system by Bednorz and Muller [51], reported in 1986, Y–Ba–C–O superconductors with T_c values slightly above 90 K were discovered. This stimulated research in four new areas: (1) the search for even higher T_c superconductors; (2) the characterization of these new high-T_c superconductors; (3) optimized processing and chemistry of the new superconductors; and (4) applications incorporating the use of these new superconductors.

The obvious potential for practical applications of high-T_c superconductivity has produced a rapid acceleration in research on this topic and, since at many agencies total research is a "zero-sum game," the new focus may have been responsible for corresponding decreases in research on other aspects of cryogenic materials (see Figure 3.4 for comparisons). The very significant advances from research on low- and high-T_c superconductors are not detailed here.

3.3.5 Other Advances

Other areas of cryogenic materials research over the same time period that, perhaps, should have been included in this review are listed here.

For ITER, the US conduit structural alloy Incoloy 908 (an age-hardened, nickel-based alloy) was developed at MIT and International Nickel Co. [52]. It has the desirable traits of matching thermal contraction to the conductor and excellent low-temperature strength, toughness, and stiffness. The alloy suffered from possible stress-accelerated oxide precipitation at the grain boundaries during the Nb_3Sn reaction treatment; considerable research was performed to minimize the effects of this trait.

The mechanical properties of the new Al–Li alloy series and its welds at low temperatures for aerospace use were extensively studied [53]. These alloys are stronger than the industry standard, i.e., 2219-T87, and their toughness is good in certain orientations. However, the grain structure of the commercial alloys is very laminated and, consequently, they tend to delaminate when tested in certain orientations.

Composites for use as structural reinforcement for cryogenic tankage or for thermal–mechanical strap or strut supports have also been studied at low temperatures [54]. For these applications, the composite-fabrication technique is usually filament winding. With filament winding, fiber tows can be oriented as desired under winding tension (to ensure straightness). Carbon, boron, S- and E-glass, and alumina fiber–epoxy matrix composites have been tested for their low-temperature properties.

3.4 General Discussion

Over the time frame considered, materials research at low temperatures has increased, but there are signs that the effort has leveled off during the past 10 years. Within this time span, superconductor R&D has steadily increased, but structural material and insulation-oriented R&D has correspondingly declined. The discovery of higher T_c superconductivity in 1986 provided the spark for increased interest in superconductors. During this time frame, the low-temperature strength and toughness of structural alloys have been improved sufficiently to meet the current needs for cryogenic applications. Research on electrical and thermal insulators has also achieved an adequate status quo, with available materials and properties to meet most application needs. There are many exceptions to these very general statements: electrical insulation materials for superconducting coils are very sensitive to radiation requirements and to coil fabrication conditions and sequence; conduit alloys for large-scale coils, such as ITER, require further R&D to justify their selection and use. Research related to space propulsion and vehicles has experienced a relative dearth of activity over the past 30 years, and R&D on thermal insulation, superconductivity, structural alloys and composites, as well as fracture control, would likely prove very productive for materials used in advanced space structures.

But, when one looks back, it is clear that the cryogenic materials community has come a long way. Reliable fracture control practices are usually in place for critical cryogenic structures. The structural alloys (austenitic steels, aluminum alloys, Fe–Ni alloys, age-hardened nickel-base alloys, and titanium alloys) are well characterized, and much experience has been gained in the joining of these alloys and in their use. We now know the important properties of most composites at cryogenic temperatures, and many glass fiber–epoxy and some carbon fiber–epoxy composites are now in use at low temperatures. Early work on thermal insulation and later R&D of electrical insulation has led to a large body of low-temperature data for these materials.

References

1. *Advances in Cryogenic Engineering (Materials)*, Vols. 22–46 (even numbers only), Plenum Press, New York, 1977–2000; vols. 48, 50, American Institute of Physics, New York, 2002, 2004.

2. Hertzberg, R.W., *Deformation and Fracture Mechanics of Engineering Materials*, John Wiley, New York, 1989.
3. Dieter, G.C., *Mechanical Metallurgy*, McGraw-Hill, New York, 1986.
4. Tada, H., Paris, P.C., and Irvin, G.R., *The Stress Analysis of Cracks Handbook*, Del Research, Hellertown, PA, 1973.
5. Shi, G.C.M., *Handbook of Stress Intensity Factors,* Lehigh University, Bethlehem, PA, 1973.
6. Murakami, Y., ed., *Stress Intensity Factors Handbook*, Pergamon Press, Oxford, 1987.
7. "Standard Test Method for Plain-Strain Fracture Toughness of Metallic Materials," Section 3, *Annual Book of ASTM Standards*, E399-90, American Society for Testing and Materials, Philadelphia, PA, 1993.
8. "Standard Test Method for $J_{Ic,}$ A Measure of Fracture Toughness," *Annual Book of ASTM Standards*, E813-89, American Society for Testing and Materials, Philadelphia, PA, 1993.
9. "Pressure Vessels," Section VIII *ASME Boiler and Pressure Vessel Code*, American Society of Mechanical Engineers, New York, 1998.
10. "Standard Test Method for Measurement of Fatigue Crack Growth Rates," *Annual Book of ASTM Standards*, American Society for Testing and Materials, Philadelphia, PA, 1993.
11. Ross, J., "Superconducting A.C. Generators Trial Rotor Forging Investigation," IRD/TM 78-47, EED/AP62/TM-174, International Research and Development Company, Ltd., Newcastle upon Tyne, England, 1978.
12. Hwang, I., "Mechanical Properties of Alcator C-MOD Superstructure Materials, Department of Materials Science and Engineering, Massachusetts Institute of Technology, Cambridge, Massachusetts, 1991.
13. Tobler, R., Berger, J., and Bussiba, A. "Long Crack Fatigue Thresholds and Short Crack Simulation at Liquid Helium Temperatures," *Advances in Cryogenic Engineering (Materials)*, Vol. 38, 1992, pp. 159–166.
14. Read, D., and Reed, R., "Fracture and Strength Properties of Selected Austenitic Stainless Steels at Cryogenic Temperatures," *Materials Studies for Magnetic Fusion Energy Applications at Low Temperatures—II*, NBSIR 79-1609, National Bureau of Standards, Boulder, Colorado, 1979, pp. 79–122.
15. Nyilas, A., Krauth, H., Metzner, M., and Munz, D., *Proc. Fatigue 84*, Second International Conference on Fatigue and Fatigue Thresholds (Birmingham, Alabama), Institut für Technische Physik, Kernforschungszentrum Karlsruhe, Germany, 1984, p. 1637.
16. Tobler, R., "Near-Threshold Fatigue Crack Growth Behavior of AISI 316 Stainless Steel," *Advances in Cryogenic Engineering (Materials)*, Vol. 32, 1986, pp. 321–328.
17. Tobler, R., and Reed, R., "Fatigue Crack Growth Rates of Structural Alloys at Four Kelvin," *NBS–ARPA Materials Research for Superconducting Machinery III*, Semi-Annual Technical Report September 1, 1974–March 1, 1975, National Bureau of Standards, Boulder, Colorado, 1975, pp. 87–104.
18. Dhers, J., Foct, J., and Vogt, J., "Influences of Nitrogen Content on Fatigue Crack Growth Rate at 77 K and 293 K of a 316L Steel," *Proc. HNS-88* (Lille, France), Institute of Metals, London, 1989, pp. 199–203.
19. Bussiba, A., Tobler, R., and Berger, J., "Superconductor Conduits, Fatigue Crack Growth Rate, and Near-Threshold Behavior of Three Alloys," *Advances in Cryogenic Engineering (Materials),* Vol. 38, 1992, pp. 167–174.
20. Reed, R., "Nitrogen in Austenitic Stainless Steels," *J. Met*. 41, 16–21, 1989.

21. Reed, R., and Simon, N., "Design of 316LN-Type Alloys," *Advances in Cryogenic Engineering (Materials)*, Vol. 34, Plenum Press, New York, 1988, pp. 165–173.
22. Reed, R., "Recent Advances in the Development of Cryogenic Steels," in *Supercollider 3*, Nonte, J., ed., Plenum Press, New York, 1991, pp. 91–106.
23. Reed, R., "Austenitic Stainless Steels with Emphasis on Strength at Low Temperatures," *Alloying*, ASM International, Materials Park, OH, 1988, pp. 225–256.
24. Reed, R., Purtscher, P., and Delgado, L., "Low-Temperature Properties of High-Manganese Steels," *High Manganese Austenitic Steels*, Lula, R., ed., ASM International, Materials Park, OH, 1988, pp. 13–21.
25. Morris, J., and Hwang, S., "Fe–Mn Alloys for Cryogenic Use: A Brief Survey of Current Research," *Advances in Cryogenic Engineering (Materials)*, Vol. 24, Plenum Press, New York, 1978, pp. 82–90.
26. Morris, J., "Structural Alloys for High Field Superconducting Magnets," *Advances in Cryogenic Engineering (Materials)*, Vol. 32, Plenum Press, New York, 1986, pp. 1–22.
27. Horiuchi, T., Ogawa, R., and Shimada, M., "Cryogenic Fe–Mn Austenitic Steels," *Advances in Cryogenic Engineering (Materials)*, Vol. 32, Plenum Press, New York, 1986, pp. 33–42.
28. Reed, R., and Horiuchi, T., eds., *Austenitic Steels at Low Temperatures,* Cryogenic Materials Series, Plenum Press, New York, 1983.
29. Simon, N., Wong, F., and Reed, R., "Metallic Material Mechanical and Thermal Property Database, Annex 1, Metallic Material Specifications for ITER Magnets," ITER EDA, Naka Joint Work Site, JAERI, Naka, Japan, 18 August 1997.
30. Shimamoto, M., Nakajima, N., Yoshida, K., and Tada, E., "Requirements for Structural Alloys for Superconducting Magnet Cases," *Advances in Cryogenic Engineering (Materials)*, Vol. 32, Plenum Press, New York, 1986, pp. 23–32.
31. Tobler, R., and Reed, R., "Interstitial Carbon and Nitrogen Effects on the Tensile and Fracture Parameters of AISI 304 Stainless Steels," *Materials Studies for Magnetic Fusion Energy Applications at Low Temperatures—III*, NBSIR 80-1627, National Bureau of Standards, Boulder, Colorado, 1980, pp. 15–48.
32. Sakamoto, T., Nakagawa, Y., Yamauchi, I., Zaizen, T., Nakajima, H., and Shimamoto, S., "Nitrogen-Containing 25Cr–13Ni Stainless Steel as a Cryogenic Structural Material," *Advances in Cryogenic Engineering (Materials)*, Vol. 30, Plenum Press, New York, 1984, pp. 137–144.
33. Takahashi, Y., Yoshida, K., Shimada, M., Tada, E. Miura, R., and Shimamoto, S., "Mechanical Evaluation of Nitrogen Strengthened Stainless Steels at 4 K," *Advances in Cryogenic Engineering (Materials)*, Vol. 28, Plenum Press, New York, 1982, pp. 73–81.
34. Reed, R., Simon, N., Purtscher, P., and Tobler, R., "Alloy 316LN for Low-Temperature Structures: A Summary of Tensile and Fracture Data," *Materials Studies for Magnetic Fusion Energy Applications at Low Temperatures—IX*, NBSIR 86-3050, National Bureau of Standards, Boulder, Colorado, 1986, pp. 15–26.
35. Stein, G., Menzel, J. and Dörr, H., "Möglichkeiten zur Herstellung von Schmiedestrücken mit hohen Stickstoffgehalten in der Desu-Anlage," *Moderne Stähle, Ergebnisse der Werkstoff-Forschung*, Vol. 1, Schweizerische Akademie der Werkstoffwissenschaften, Zurich, 1987, pp. 181–193.
36. Uggowitzer, P., and Harzenmoser, M., "Strengthening of Austenitic Stainless Steels by Nitrogen," *Proc. HNS–88* (Lille, France), Institute of Metals, London, 1989, pp. 175–179.
37. Reed, R., and Golda, M., "Properties of Cold-to-Warm Support Straps," *Cryogenics* 38, 39–42, 1998.

38. Reed, R., and Golda, M., "Cryogenic Composite Supports: A Review of Strap and Strut Properties," *Cryogenics* 37, 233–250, 1997.
39. Kasen, M., MacDonald, G., Beekman, D., and Schramm, R., "Mechanical, Electrical, and Thermal Characterization of G-10CR and G-11CR Glass-Cloth/Epoxy Laminates between Room Temperature and 4 K," *Advances in Cryogenic Engineering (Materials)*, Vol. 26, Plenum Press, New York, 1980, pp. 235–244.
40. Benzinger, J., "Manufacturing Capabilities of CR-grade Laminates," *Advances in Cryogenic Engineering (Materials)*, Vol. 36, Plenum Press, New York, 1980, pp. 252–258.
41. Reed, R., Fabian, P., and Schutz, J., "Turn Insulation for U.S. CS Model Coil," U.S. ITER Insulation Program for Plasma Science and Fusion Center, Massachusetts Institute of Technology, Cambridge, Massachusetts, 1 March 1998.
42. Reed, R., and Clark, P., "Vacuum Pressure Impregnation of U.S. CS Model Coil," US ITER Insulation Program for Plasma Science and Fusion Center, Massachusetts Institute of Technology, Cambridge, MA, 31 March 1999.
43. Simon, N., Reed, R., and Walsh, R., "Compression and Shear Tests of Vacuum-Impregnated Composites," *Advances in Cryogenic Engineering (Materials)*, Vol. 38A, Plenum Press, New York, 1992, pp. 363–370.
44. Fabian, P., Munshi, N., Feucht, S., Bittner, K., Rohrhofer, X., Huner, K., and Weber, H., "Low Temperature Mechanical Properties of Cyanate Ester Insulation Systems after Irradiation," *Advances in Cryogenic Engineering (Materials)*, Vol. 50A, American Institute of Physics, Mellville, NY, 2004, pp. 289–296.
45. Codell, D., and Fabian, P., "Development of Pre-preg Ceramic Insulation for Superconducting Magnets," *Advances in Cryogenic Engineering (Materials)*, Vol. 50A, American Institute of Physics, Mellville, NY, 2004, pp. 259–265.
46. Puigsegur, A., Rondeaux, F., Prouzet, E., and Samoogabalan, K., "Development of an Innovative Insulation for Nb_3Sn Wind and React Coils," *Advances in Cryogenic Engineering (Materials)*, Vol. 50A, American Institute of Physics, Mellville, NY, 2004, pp. 266–272.
47. Bata, F., Hascicek, Y., Sumption, M., Arda, L., Aslanoglu, Z., Akin, Y., and Collings, E., " A Sol–Gel Approach to the Insulation of Rutherford Cables," *Advances in Cryogenic Engineering (Materials)*, Vol. 50A, American Institute of Physics, Mellville, NY, 2004, pp. 273–280.
48. Zeller, A., "Anodized Insulation for CICC Coils," *Advances in Cryogenic Engineering (Materials)*, Vol. 48A, American Institute of Physics, Melville, NY, 2002, pp. 255–260.
49. Reed, R., Fabian, P., and Schutz, J., "U.S. ITER Insulation Irradiation Program," Final Report to Plasma Fusion Center, Massachusetts Institute of Technology, Cambridge, MA, 31 August 1995.
50. Reed, R., Fabian, P., and Schutz, J., "U.S. ITER Insulation Irradiation Program, Final Report to Plasma Fusion Center, Massachusetts Institute of Technology, Cambridge, Massachusetts, 31 August 1995.
51. Bednorz, J., and Muller, K., "Possible High-T_c Superconductivity in the Ba–La–Cu–O System," *Z. Phys. B*, 64, 189, 1986.
52. Hwang, I., Ballinger, R., Morra, M., and Steeves, M., "Mechanical Properties of Incoloy 908—An Update," *Advances in Cryogenic Engineering (Materials)*, Vol. 38, Plenum Press, New York, 1992, pp. 1–10.
53. Simon, N., Drexler, E., and Reed, R., *Review of Cryogenic Mechanical and Thermal Properties of Al–Li Alloys and Alloy 2219*, NISTIR 3971, National Institute of Standards and Technology, Boulder, Colorado, 1991.
54. Hartwig, G., "Status and Future of Fibre Composites," *Advances in Cryogenic Engineering (Materials)*, Vol. 40, Plenum Press, New York, 1994, pp. 961–975.